

1  
2  
3  
4  
5  
6  
7  
8  
9  
10  
11  
12  
13  
14  
15  
16  
17  
18  
19  
20  
21  
22  
23  
24  
25  
26  
27  
28  
29  
30  
31  
32  
33  
34  
35  
36  
37  
38  
39  
40  
41  
42  
43  
44

**The Active Fracture Model:  
Its Relation to Fractal Flow Patterns and a Further Evaluation using Field  
Observations**

Hui-Hai Liu, Guoxiang Zhang, and Gudmundur S. Bodvarsson  
Earth Sciences Division  
Lawrence Berkeley National Laboratory  
Berkeley, California

Submitted to *Vadose Zone Journal*

1 **ABSTRACT**

2

3 The active fracture model (AFM) (Liu et al., 1998) has been widely used in modeling  
4 flow and transport in the unsaturated zone of Yucca Mountain, Nevada, a proposed  
5 repository of high-level nuclear wastes. This study presents an in-depth evaluation of the  
6 AFM, based on both theoretical arguments and field observations. We first argue that  
7 flow patterns observed from different unsaturated systems (including the unsaturated  
8 zone of Yucca Mountain) may be fractals. We derive an interesting relation between the  
9 AFM and the fractal flow behavior, indicating that the AFM essentially captures this  
10 important flow behavior at a subgrid scale. Finally, the validity of the AFM is  
11 demonstrated by the favorable comparison between simulation results based on the AFM  
12 and C-14 age and fracture coating data collected from the unsaturated zone at Yucca  
13 Mountain. These data sets independently provide important insight into flow and  
14 transport processes at the Yucca Mountain site. Potential future improvements of the  
15 AFM include expanding it to consider film flow and multifractal concepts.

1 Flow and transport in unsaturated fractured rocks are generally complicated because  
2 of the complexity of fracture-matrix interaction mechanisms, distinct differences in  
3 hydraulic properties between fractures and the matrix, and nonlinearity involved in  
4 unsaturated flow. Recently, the investigation into using the unsaturated zone at Yucca  
5 Mountain, Nevada, as a storage facility for the geological disposal of high-level nuclear  
6 wastes has generated intensive research interests in modeling flow and transport in  
7 unsaturated fractured rocks (e.g., Bodvarsson and Tsang, 1999; Robinson et al. 1997;  
8 Pruess et al., 1999; Liu et al. 1998; Ho, 1997). To reliably assess the performance of the  
9 repository, it is desirable to accurately predict flow and transport processes within the  
10 mountain. Modeling flow and transport in unsaturated fractured rocks is also of interest in  
11 other areas including environmental contamination in arid and semiarid regions.

12 Several approaches are available in the literature for modeling flow and transport in  
13 unsaturated fractured rocks. When classified according to the manner in which fracture  
14 networks are treated in the model structure, these approaches mainly fall into one of the  
15 two categories: the continuum approach and the discrete fracture network approach.  
16 Excellent reviews on these approaches, which have been developed and used in different  
17 fields (including oil reservoir engineering, groundwater hydrology, geothermal  
18 engineering and soil physics), can be found in Bear et al. (1993), National Research  
19 Council (1996) and Pruess et al. (1999).

20 In the continuum approach, fractures are considered to be sufficiently ubiquitous and  
21 distributed in such a manner that they can be meaningfully described statistically (Bear et  
22 al., 1993). The role of individual fractures in fractured media is considered to be similar  
23 to that of individual pores in porous media. Therefore, one can describe average fracture

1 properties as macroscopic and those associated with individual fractures as microscopic.  
2 In the continuum approach, connected fractures and rock matrix are viewed as two or  
3 more overlapped interacting continua. In other words, at a “point,” two or more continua  
4 are considered to co-exist. In this case, the continuum mechanics formulations, such as  
5 those used for porous media, can be used to describe flow and transport in each  
6 continuum. Coupling of processes between different continua is determined by their  
7 interaction mechanisms at a subgrid scale.

8 The fracture network approach involves the generation, by computer simulation, of  
9 synthetic fracture networks, and the subsequent modeling of flow and transport in these  
10 networks. The approach has been extensively used for single-phase flow and transport,  
11 with deterministic, stochastic, artificial, or site-specific fracture networks (e.g., Bear et al.  
12 1993; National Research Council, 1996), and has recently been applied to unsaturated  
13 conditions (Rasmussen, 1991; Kwicklis and Healey, 1993; Karasaki et al. 1994;  
14 Zimmerman and Bodvarsson, 1996; Liu and Bodvarsson, 2001; Liu et al., 2003a).

15 Both continuum and fracture network approaches have advantages and disadvantages.  
16 While the fracture network approach is useful as a tool for concept evaluation or model-  
17 based process studies, it has several limitations. First, the approach requires geometric  
18 parameters that may strongly impact flow and transport, such as fracture apertures and  
19 conductivity, but typically cannot be well constrained from field observations (Pruess et  
20 al., 1999). Second, it is difficult to separate the conductive fracture geometry from the  
21 non-conductive fracture geometry (National Research Council, 1996). Third, flow and  
22 transport models based on the approach can be complex and computationally intensive  
23 for realistic fracture densities (National Research Council, 1996). Fourth, so far, the

1 studies based on the fracture network approach have rarely considered fracture-matrix  
2 interaction (flow and transport between fractures and the matrix), because of  
3 computational intensity for unsaturated flow and transport (Pruess et al., 1999). The  
4 fracture-matrix interaction has important effects on flow and transport processes in  
5 unsaturated fractured rocks. Because the continuum approach is relatively simple and  
6 straightforward to implement, it is preferred for most applications encountered in practice  
7 (National Research Council, 1996). For example, because the number of fractures is on  
8 the order of  $10^9$  at Yucca Mountain (Doughty, 1999), it is practically impossible to  
9 construct and calibrate a discrete fracture network site-scale model with so many  
10 fractures, considering data availability and computational feasibility. Therefore, the dual-  
11 continuum approach, in which fractures and the matrix are treated as two overlapping and  
12 interactive continua, has been used as the baseline approach for modeling flow and  
13 transport within Yucca Mountain (Bodvarsson and Tsang, 1999; Liu, 2000). Note that a  
14 similar approach has also been used to model unsaturated flow and transport in structured  
15 soils (Gerke and van Genuchten, 1993).

16 A traditional continuum approach assumes uniformly distributed flow patterns at a  
17 subgrid scale and therefore cannot be used for representing gravity-driven fingering flow  
18 and transport in fracture networks, resulting from subsurface heterogeneities and  
19 nonlinearity involved in unsaturated flow (Glass, 1996; Liu et al., 1998; Sue et al., 1999;  
20 Pruess et al., 1999). In an effort to incorporate this flow behavior into the continuum  
21 approach, Liu et al. (1998) developed an active fracture model (AFM) that assumes only  
22 a portion of fractures in a connected unsaturated fracture network to contribute to liquid  
23 water flow. Because the AFM can provide a large range of flow behaviors in unsaturated

1 fractures (including fast flow behavior), it has been used extensively for modeling large-  
2 scale flow and transport in the unsaturated zone of Yucca Mountain (e.g., Moridis and Hu,  
3 2000; Wu et al., 2000; Wu et al., 2002; Liu et al., 2003b; Zhou et al., 2003; Buscheck et  
4 al., 2002; Xu et al., 2003).

5 While previous studies have shown that simulation results based on the AFM are  
6 generally consistent with field observations from the unsaturated zone of Yucca  
7 Mountain (Liu et al., 1998; Liu et al., 2003b), a more in-depth evaluation of the AFM is  
8 highly desirable, because accurately modeling complex, large-scale flow and transport  
9 within unsaturated fractured rocks is of interest to many research areas. Therefore, the  
10 major objective of this work is to provide a further evaluation of the AFM, based on both  
11 theoretical arguments and field observations. In this paper, we first show that flow  
12 patterns in unsaturated systems (including the unsaturated zone of Yucca Mountain) may  
13 be characterized by fractals. Then we will show that the AFM is approximately consistent  
14 with fractal flow patterns at the subgrid scale. Finally, we demonstrate that simulation  
15 results based on the AFM can represent different data sets collected from the Yucca  
16 Mountain site. These data sets contain important information about large-scale flow and  
17 transport processes at the site.

## 18 **ACTIVE FRACTURE MODEL**

19 The AFM was developed within the context of the dual-continuum approach (Liu et  
20 al., 1998). While the details of the AFM can be found in Liu et al. (1998), a brief  
21 introduction of the AFM is provided here for convenience. The active fracture concept is  
22 based on the reasoning that, because of the fingering flow, only a portion of fractures in a

1 connected, unsaturated fracture network contribute to liquid water flow, while other  
2 fractures are simply bypassed. The portion of the connected fractures that actively  
3 conduct water are called active fractures. We hypothesize that the number of active  
4 fractures in the unsaturated zone of Yucca Mountain is small compared to the total  
5 number of connected fractures such that active fractures, rather than total connected  
6 fractures, must be used in numerical models. We further hypothesize that the number of  
7 active fractures within a gridblock is large; hence, the continuum approach is still valid  
8 for describing fracture flow. These hypotheses are consistent with the consideration that  
9 fractures conducting water in the unsaturated zone of Yucca Mountain are many and  
10 highly dispersed (Liu, 2000).

11 To use the active fracture concept for modeling flow and transport in fractures, we  
12 treat active fractures as a portion of the “homogeneous” fracture continuum for a given  
13 gridblock. Note the differences between the active fracture model and the conventional,  
14 capillary-equilibrium-based, fracture-water distribution model. The latter assumes that  
15 liquid water occupies first fractures with small apertures, and then fractures with  
16 relatively large apertures, as water potential (or water saturation) increases. In contrast,  
17 the active fracture model presumes gravity-dominated, nonequilibrium, preferential liquid  
18 water flow in fractures, which is expected to be similar to fingering flow in unsaturated  
19 porous media. A liquid finger can bypass a large portion of a porous medium, which does  
20 not necessarily correspond to large pores. Note that the above discussion is valid for  
21 large-scale flow processes and not inconsistent with possible validity of a capillary-  
22 equilibrium-based water distribution concept at relatively small scales corresponding to  
23 an individual flow path or a single flow finger.

1 Flow and transport conditions and fractured rock properties should determine the  
2 fraction of active fractures in a connected fracture network,  $f_a$ . An expression for  $f_a$  must  
3 satisfy the following conditions: all connected fractures are active ( $f_a = 1$ ) if the system is  
4 fully liquid saturated; all fractures are inactive ( $f_a = 0$ ) if the system is at residual  
5 saturation; and  $f_a$  should be related to water flux in fractures. It is generally believed that  
6 more fractures are conducive to a larger water flux. This water flux in fractures is  
7 considered to be mainly dependent on fracture saturation because fracture water flow is  
8 gravity-dominated. A simple expression for  $f_a(-)$ , which meets these conditions and  
9 includes only one parameter, is a power function of effective water saturation in  
10 connected fractures,  $S_e(-)$ :

$$11 \quad f_a = S_e^\gamma \quad [1]$$

12  
13 where  $\gamma (-)$  is a positive constant depending on properties of the corresponding fracture  
14 network, and the effective water saturation in connected fractures is given by

$$15 \quad S_e = \frac{S_f - S_r}{1 - S_r} \quad [2]$$

16  
17 where  $S_f(-)$  is the water saturation of all connected fractures and  $S_r$  is the residual fracture  
18 saturation. In this study, Eq. [1] is used to determine the fraction of active fractures. As  
19 will be discussed below, this simple equation is actually the first-order approximation for  
20 fractal flow behavior at a subgrid scale, although it was initially developed as an  
21 empirical relation (Liu et al., 1998).

1 Note that only the active fracture continuum, a portion of the total fracture continuum,  
2 contributes to flow and transport in fractures and fracture-matrix interaction. Fracture  
3 hydraulic properties should thus be defined for active fractures. The effective water  
4 saturation of active fractures,  $S_{ae}(-)$ , is related to the effective water saturation in  
5 connected fractures,  $S_e$ , by

$$6 \quad S_{ae} = \frac{S_e}{f_a} = S_e^{1-\gamma} \quad [3]$$

7  
8 Because  $S_{ae} \leq 1$ ,  $\gamma$  should be smaller than or equal to one. The effective water saturation  
9 of active fractures is related to the actual water saturation in active fractures,  $S_a$ , by

$$10 \quad S_{ae} = \frac{S_a - S_r}{1 - S_r} \quad [4]$$

11  
12 If all connected fractures are considered to be active in conducting water, as assumed in  
13 previous studies, the water capillary pressure for the fracture continuum may be  
14 described by the well-known van Genuchten relation (van Genuchten 1980):

$$15 \quad P_c(S_e) = \frac{1}{\alpha} [S_e^{-1/m} - 1]^{1/n} \quad [5]$$

16  
17 where  $\alpha$ , ( $\text{Pa}^{-1}$ ),  $n$ , (-) and  $m=1-1/n$  are van Genuchten parameters. In the active fracture  
18 model, however, the van Genuchten capillary-pressure relation is considered to be  
19 relevant for the active fracture continuum, rather than for the whole fracture continuum.

1 The capillary pressure for active fractures is determined by replacing  $S_e$  in Eq. [5] with  
 2  $S_{ae}$ :

$$3 \quad P_c(S_e) = \frac{1}{\alpha} [S_{ae}^{-1/m} - 1]^{1/n} = \frac{1}{\alpha} [S_e^{(\gamma-1)/m} - 1]^{1/n} \quad [6]$$

4

5 Eq. [6] rather than [5] should be used to simulate water flow in the fracture continuum.  
 6 For a given effective water saturation in connected fractures, a larger  $\gamma$  value corresponds  
 7 to a larger effective water saturation in active fractures, and therefore to a lower absolute  
 8 value for capillary pressure.

9 The liquid-phase relative permeability for the active fracture continuum,  $k_{ar}(-)$ , is  
 10 directly determined by the effective water saturation of active fractures. However,  
 11 because only a portion of the fractures are active, the relative permeability of the entire  
 12 fracture continuum,  $k_r(-)$  should be the relative permeability of active fractures  
 13 multiplied by  $f_a$ , or

$$14 \quad k_r = f_a k_{ar} = S_e^\gamma k_{ar} \quad [7]$$

15

16 where  $k_{ar}$  can be given by the following van Genuchten permeability relation:

$$17 \quad k_{ar} = S_{ae}^{1/2} [1 - \{1 - S_{ae}^{1/m}\}^m]^2 = S_e^{(1-\gamma)/2} [1 - \{1 - S_e^{(1-\gamma)/m}\}^m]^2 \quad [8]$$

18 Combining Eqs. [7] and [8] yields

$$19 \quad k_r = S_e^{(1+\gamma)/2} [1 - \{1 - S_e^{(1-\gamma)/m}\}^m]^2 \quad [9]$$

1 In general, relative permeability ( $k_r$ ) is affected by  $\gamma$  in a complicated manner for a given  
2  $S_e$ . A larger  $\gamma$  value, resulting in a higher effective water saturation in active fractures  
3 ( $S_{ae}$ ), gives rise to a larger value of  $k_{ar}$ . On the other hand, a larger  $\gamma$  value corresponds to  
4 a smaller value of  $f_a$ . Because the former effect is dominant, a larger  $\gamma$  value gives a  
5 larger relative permeability for a given effective water saturation of the fracture  
6 continuum.

7 Note that the van Genuchten relationships were developed for porous media rather  
8 than fracture networks. Recently, Liu and Bodvarsson (2001) developed a new  
9 constitutive-relationship model for unsaturated flow in fracture networks, based mainly  
10 on numerical experiments. They found that the van Genuchten model is approximately  
11 valid for low fracture saturations corresponding to the ambient conditions in the  
12 unsaturated zone of Yucca Mountain. Therefore, the van Genuchten relationships are  
13 still employed because it is the ambient flow process that is of interest here. However, we  
14 emphasize that the key hypothesis of the AFM is Eq. [1]. This equation can be combined  
15 with any appropriate constitutive-relationship model to simulate unsaturated flow  
16 processes in fractured porous media. Consequently, the focus of this work is on  
17 evaluation of Eq. [1].

18 In an unsaturated fracture network, the ratio of the interface area contributing to  
19 flow and transport between fractures and the matrix, to the total interface area determined  
20 geometrically from the fracture network, is called the fracture-matrix interface area  
21 reduction factor. In the active fracture model, this reduction factor results from three  
22 considerations. First, the average interface area between mobile water in an active

1 fracture and the surrounding matrix is smaller than the geometric interface area. Second,  
2 the number of active fractures is smaller than that of connected fractures. (Conventionally,  
3 all connected fractures are assumed to contribute to fracture-matrix interaction). Third,  
4 average active fracture spacing is much larger than that for connected fractures. Under  
5 the quasi-steady-state condition, flow and transport between fractures and surrounding  
6 matrix is inversely proportional to the corresponding fracture spacing. Based on these  
7 considerations, Liu et al. (1998) derived an expression for the reduction factor:

$$8 \quad R \cong S_e^{1+\gamma} \quad [10]$$

9  
10 In summary, the active fracture model uses a combination of the volume-averaged  
11 method and a simple filter to deal with fracture flow and transport. Inactive fractures are  
12 filtered out in modeling fracture-matrix interaction, flow, and transport in the fracture  
13 continuum. The  $\gamma$  factor may be interpreted as a measure of the “activity” of connected  
14 fractures. Generally speaking, a smaller  $\gamma$  value corresponds to a larger number of active  
15 fractures in a connected fracture network. For example,  $\gamma = 0$  results in  $f_a = 1$  in Eq. [1],  
16 corresponding to all connected fractures being active. On the other hand,  $\gamma = 1$   
17 corresponds to zero fracture capillary pressure (Eq. [6]), indicating that all active  
18 fractures are saturated. In the latter case, the fraction of active fractures is very small for  
19 small percolation fluxes, because relatively high fracture permeabilities allow most of the  
20 water to flow through only a few fractures.

21

22

# 1 THE AFM AND FRACTAL FLOW BEHAVIOR IN UNSATURATED SYSTEMS

2 A flow system exhibits so-called fractal flow behavior when the corresponding flow  
3 patterns can be characterized by fractals. In this section, a brief discussion of fractal  
4 dimension (used for characterizing fractal patterns) is presented, followed by a discussion  
5 of evidence for fractal flow behavior in unsaturated systems and relations between the  
6 AFM and this fractal flow behavior.

## 7 Fractal Dimension

8 Fractal dimension,  $d_f$ , is generally a noninteger and less than the corresponding  
9 Euclidean (topological) dimension of a space,  $D$ . Different kinds of definitions of fractal  
10 dimension exist (e.g., similarity dimension, Hausdorff dimension, and box dimension),  
11 although they provide very close fractal dimension values for practical applications  
12 (Feder, 1988). The most straightforward definition is the so-called box dimension, based  
13 on a simple “box-counting” procedure. This dimension is determined from Eq. [11]  
14 (below) by counting the number ( $N$ ) of “boxes” (e.g., line segment, square and cubic for  
15 one-, two-, and three-dimensional problems, respectively), needed to cover a spatial  
16 pattern, as a function of the box size ( $l$ ) (e.g., Feder, 1988):

$$18 \quad N(l) = \left(\frac{L}{l}\right)^{d_f} \quad [11]$$

19  
20 where  $L$  refers to the size of the entire spatial domain under consideration. Figure 1  
21 shows a box-counting procedure for a spatial pattern with  $d_f = 1.6$ , in a two-dimensional

1 domain with size  $L$  (Yamamoto et al., 1993).

2

3 Obviously, if a spatial pattern is uniformly distributed in space, the fractal dimension  
4 will be identical to the corresponding Euclidean dimension. In this case, the box number,  
5  $N^*$ , and the box size  $l$  have the following relation

6

$$7 \quad N^*(l) = \left(\frac{L}{l}\right)^D \quad [12]$$

8 A fractal pattern exhibits similarity at different scales. When  $d_f < D$ , the corresponding  
9 pattern does not fill the whole space, but only part of it (Fig. 1).

## 10 **Fractal Flow Behavior in Unsaturated Systems**

11 Fractals have been shown to provide a common language for describing many  
12 different natural and social phenomena (Mandelbrot, 1982). While a vast literature exists  
13 on the validity of the fractal concept for a great number of fields, fractals have been  
14 found to be useful for representing many spatial distributions in subsurface hydrology,  
15 including soil particle size distribution, roughness of fracture surface, distribution of  
16 permeability in heterogeneous formations, and large-scale solute dispersion processes  
17 (e.g., Tyler and Wheatcraft, 1990; Rieu and Sposito, 1991a, b; Perfect et al., 1996;  
18 Neuman, 1990, 1994; Molz and Boman, 1993; Molz et al., 1997). Especially, recent  
19 studies have suggested that complex flow (or solute transport) patterns in unsaturated  
20 systems can be characterized by fractals (below).

21

22 Flury and Flühler (1995) first indicated that solute leaching patterns, observed from  
23 three field plots consisting of an unsaturated loamy soil, could be well represented by a

1 diffusion-limited aggregation (DLA) model (Witten and Sander, 1981), although the  
2 relation between DLA parameters and soil hydraulic properties is still an unresolved issue.  
3 It has been documented that DLA generates fractal patterns (e.g., Feder, 1988; Flury and  
4 Flühler, 1995). The observation of Flury and Flühler (1995) is further supported by a  
5 study of Persson et al. (2001), who used dye-infiltration data to investigate field pathways  
6 of water and solutes under unsaturated conditions. Persson et al. (2001) showed that field  
7 observations are well described by the DLA model. Furthermore, they demonstrated that  
8 observed mean power spectrum for dye penetration of a field plot displays a typical  
9 power-law relationship, another important indication of fractal flow behavior. Glass  
10 (1993) first showed that unsaturated flow in a single vertical fracture is characterized by  
11 gravity-driven fingers, and the resulting flow patterns could be modeled by an invasion-  
12 percolation approach (Wilkinson and Wilemsen, 1983). Again, percolation-based models  
13 generate fractal clustering patterns (Stauffer and Aharony, 2001). Closely related to flow  
14 and transport processes in unsaturated systems, flow patterns observed from multiphase  
15 systems are also related to fractals. For example, viscous fingering in porous media has  
16 been experimentally shown to be fractal (Feder, 1988). The problem of viscous fingering  
17 in porous media is of central importance in oil recovery. Smith and Zhang (2001) also  
18 reported that DNAPL fingering in water saturated porous media, observed from sandbox  
19 experiments, is fractal.

20

21 Detailed experimental studies on unsaturated flow patterns in large-scale fracture  
22 networks are scarce in the literature, because of the technical difficulties in observing  
23 these patterns in the field. Fortunately, some geochemical data sets closely related to flow

1 patterns in large-scale fracture networks have recently become available from the  
2 unsaturated zone of Yucca Mountain. For example, a spatial distribution of fractures with  
3 mineral coatings was determined along an underground tunnel, using a detailed-line-  
4 survey method (Paces et al., 1996; Fabryka-Martin et al. 2000). The total survey length  
5 along the tunnel is several thousand meters, broken up by a number of disconnected 30 m  
6 survey intervals. As will be discussed below, fracture coating is roughly a signature of  
7 water flow paths. Therefore, this data set can be used to infer potential fractal flow  
8 behavior at a large fracture-network scale.

9

10 While the detailed line survey was performed for several geological units, we focus on  
11 the one that is densely fractured (average fracture spacing is about 0.2 m) and has the  
12 largest number of 30 m survey intervals. In this unit, about 130 coated fractures were  
13 found over the approximate 1,000 m survey length. The intersections of coated fractures  
14 with the survey line (along the underground tunnel) form a set of points. If the  
15 corresponding flow pattern is fractal, the point set should be fractal too. A box-counting  
16 method is used to detect the fractal pattern from this point set. Fig. 2 shows number of  
17 boxes (line segments),  $N$ , covering at least one intersection point as a function of box size  
18 (length of a segment),  $l$ . Note that the largest box size corresponds to the length of survey  
19 intervals (30 m). The smallest box size used here is 3 m. If all fractures are coated, all  
20 boxes of this size or larger should at least cover one of the intersection points, because  
21 the average fracture spacing is much smaller than this size. This corresponds to a  
22 dimension of one (the topological dimension) based on Eq. [11].

23

1

2 Fig. 2 shows that the data points can be fitted by a power function with a power of  $-0.5$ ,  
3 indicating the existence of a fractal pattern for coated fractures (or flow paths). The  
4 power value suggests a fractal dimension of  $0.5$  that is not an integer but smaller than the  
5 corresponding topological dimension (one). To the best of our knowledge, the fractal  
6 flow behavior in large-scale unsaturated fracture networks, observed from field data, has  
7 not been previously reported in the literature. While more studies may be needed to  
8 further confirm the finding reported here, it is generally reasonable to expect the  
9 existence of fractal flow behavior in large-scale unsaturated fracture networks, given the  
10 evidence shown here and the fact that complex unsaturated flow patterns in several  
11 different natural systems are fractals (and fractals are valid for describing many different  
12 processes).

13

#### 14 **A Relation between the AFM and Fractal Flow Patterns**

15 We have shown that flow processes in unsaturated systems (including fracture networks)  
16 may be fractal. This has many important implications regarding the development of  
17 numerical models for large-scale unsaturated systems, because fractal patterns are  
18 generally related to fingering and/or preferential flow paths. In this section, we will  
19 demonstrate the AFM's consistency with fractal flow behavior in unsaturated fracture  
20 networks.

21

22 Consider Fig. 1(a) to be a gridblock containing a fracture network and the  
23 corresponding flow pattern in the fracture network to be fractal. In this case, only a

1 portion of the medium within a gridblock contributes to water flow (Fig. 1). This is  
 2 conceptually consistent with the AFM (Liu et al. 1998). Note that in Fig. 1, a box is  
 3 shadowed if it covers one or more fractures (or fracture segments) that conduct water. For  
 4 simplicity, further consider that fractures are randomly distributed in space, and thus the  
 5 dimension for water-saturation distribution is the corresponding Euclidean dimension  
 6 when all the connected fractures actively conduct water. As will be obvious from the  
 7 derivations to follow, this assumption does not alter our general conclusion regarding the  
 8 connection between the AFM and fractal flow patterns.

9

10 Combining Eqs. [11] and [12] yields

11

$$12 \quad [N(l)]^{1/d_f} = [N^*(l)]^{1/D} \quad [13]$$

13

14 The average water saturation ( $S_e$ ) for the whole gridblock (Fig. 1(a)) is determined to be

15

$$16 \quad S_e = \frac{V}{l^D \phi N^*(l)} \quad [14]$$

17 where  $V$  is the total water volume (excluding residual water) in fractures within the

18 gridblock (Fig. 1a), and  $\phi$  is fracture porosity. Similarly, the average water saturation ( $S_b$ )

19 for shadowed boxes with a size of  $l$  is

20

$$21 \quad S_b = \frac{V}{l^D \phi N(l)} \quad [15]$$

1 From Fig. 1, it is obvious that there exists a box size  $l_1 < L$  satisfying:

$$2 \quad \frac{V}{l_1^D \phi} = 1 \quad [16]$$

3 Based on Eqs. [13]–[16], the average saturation for shadowed boxes with size  $l_1$ ,  $S_{b1}$ , can  
4 be expressed by

$$5 \quad S_{b1} = (S_e) \frac{df}{D} \quad [17]$$

7 Because a fractal is similar at different scales, the procedure to derive Eq. [17] from  
8 a gridblock with size  $L$  can be applied to shadowed boxes with the smaller size of  $l_1$ . In  
9 this case, for a given box size smaller than  $l_1$ , the number of shadowed boxes will be  
10 counted as an average number for those within the (previously shadowed) boxes with a  
11 size of  $l_1$ . Again, we can find a box size  $l_2 < l_1$  to obtain a saturation relation:

$$12 \quad S_{b2} = (S_{b1}) \frac{df}{D} = (S_e) \left( \frac{df}{D} \right)^2 \quad [18]$$

13

14 The procedure to obtain Eq. [18] can be continued until it reaches an iteration level,  $n^*$ ,  
15 at which all the shadowed boxes with a size of  $l_n$  cover active fractures only. The  
16 resultant average saturation for these shadowed boxes is

$$17 \quad S_{bn} = (S_e) \left( \frac{df}{D} \right)^{n^*} \quad [19]$$

18 By definition of active fractures,  $S_{bn}$  should be equivalent to the effective saturation  
19 of active fractures. It is remarkable that Eq. [19] is similar to Eq. [3], obtained from a key  
20 hypothesis of the AFM that the fraction of active fractures in an unsaturated fracture

1 network is a power function of the average effective saturation of the network.  
2 Comparing these two equations yields:

3

$$4 \quad \gamma = 1 - \left( \frac{d_f}{D} \right)^{n^*} \quad [20]$$

5 Eq. [20] provides the first theoretical relation between the AFM parameter  $\gamma$  and the  
6 fractal dimension, while  $\gamma$  was initially developed as an empirical parameter (Liu et al.,  
7 1998). Thus, the AFM essentially captures fractal flow behavior at the gridblock scale ( $d_f$   
8  $< D$ ), whereas traditional continuum approaches assume a uniform flow pattern (or  
9 effective-saturation distribution) at that scale (corresponding to  $d_f = D$  or  $\gamma = 0$ ). In other  
10 words, the AFM can be used for simulating fractal flow behavior (in an unsaturated  
11 fracture network) that cannot be handled by traditional continuum approaches.

12

### 13 **A Preliminary Assessment of Saturation Dependency of the AFM Parameter $\gamma$**

14

15 Eq. [20] implies that the AFM parameter  $\gamma$  is not a constant, as assumed by Liu et al.  
16 (1998), but a function of saturation (or other flow conditions), because both iteration  
17 level  $n^*$  and  $d_f$  may be dependent on water saturation for a given fracture network. The  
18 relations among  $n^*$ ,  $d_f$ , and the relevant flow conditions (such as saturation) are not  
19 totally clear at this point. However, a constant  $\gamma$  is a reasonable treatment at least for a  
20 limited range of water saturations (or flow conditions), which is the case for the  
21 unsaturated zone of Yucca Mountain where the fracture saturation is believed to be  
22 typically less than 10% under ambient conditions. On the other hand, experimental

1 evidence seems to indicate that  $\gamma$  is a weak function of saturation at least for porous  
2 media under certain conditions (which will be discussed below). It is obvious from the  
3 derivation of Eq. [20] that the AFM concept and Eq. [20] can be applied to porous media  
4 also, as long as fingering flow patterns in them are fractals. With this in mind, results  
5 from porous media may be used to conceptually evaluate the relation between  $\gamma$  and  
6 water saturation for unsaturated fracture networks.

7

8 Based on laboratory experimental observations reported in the literature, Wang et al.  
9 (1998) derived a relation between flow conditions and a parameter,  $F$ , defined as the ratio  
10 of horizontal cross-sectional area occupied by gravity fingers, to the total cross-sectional  
11 area.  $F$  corresponds to  $f_a$  that is defined as the portion of active fractures in a fracture  
12 network (Eq.[1]). Wang et al. (1998) related  $F$  to the ratio of average water flux through  
13 the whole cross-sectional area,  $q$ , to the saturated hydraulic conductivity of the porous  
14 medium,  $K_s$ , as follows:

$$15 \quad F \approx \left( \frac{q}{K_s} \right)^{1/2} \quad [21]$$

16 for  $q/K_s = 0.4 - 1.0$ . By definition, we can relate the average water flux within fingers  
17 ( $q_F$ ) to  $q$  by

$$18 \quad q_F = \frac{q}{F} \quad [22]$$

19 and also relate the average water saturation of fingers,  $S_F$ , to the average water saturation  
20 for the whole cross-sectional area,  $S_e$ , by

$$21 \quad S_F = \frac{S_e}{F} \quad [23]$$

1 It is expected that flow within a gravitational finger is gravity dominated. In this case, we  
2 can approximately have

$$3 \frac{q_F}{K_s} \approx k_r = S_F^\beta \quad [24]$$

4 Eq. [24] uses the Brooks-Corey (1964) model for describing relationship between relative  
5 permeability ( $k_r$ ) and saturation relationship, with  $\beta$  a constant. Combining Eqs. [21] to  
6 [24] yields

$$7 F \approx (S_e)^{\frac{\beta}{1+\beta}} \quad [25]$$

8 Comparing the above equation with Eq. [1] gives

$$10 \gamma \approx \frac{\beta}{1+\beta} \quad [26]$$

11 Therefore,  $\gamma$  is a constant under certain conditions for porous media. Consequently, we  
12 expect that  $\gamma$  may be a weak function of saturation for unsaturated fracture networks if  
13 fingering flow patterns in a porous medium are considered to be analogous to flow  
14 patterns in the networks. However, we acknowledge that this connection needs more  
15 investigation in future studies.

16

## 17 **EVALUATION OF THE AFM USING FIELD OBSERVATIONS**

18

19 So far, we have shown that fractal flow behavior may be common in different  
20 unsaturated systems (including unsaturated fracture networks) and also that the AFM is,  
21 in general, consistent with this behavior. In this section, we will further evaluate the AFM

1 using different data sets collected from the Yucca Mountain site. Considering the  
2 complexity of large-scale unsaturated flow and transport in fractured porous media, the  
3 direct use of actual field data for evaluating a model is critical. Previously, it has been  
4 shown that simulation results based on the AFM match the matrix saturation and water  
5 potential data collected from long boreholes at the Yucca Mountain site (e.g., Liu et al.,  
6 1998). These results are also consistent with flow and tracer transport data observed from  
7 a field test (on a scale of about 20 m) performed in a densely fractured unit within Yucca  
8 Mountain (Liu et al., 2003b). In this study, we focus on evaluating the AFM with C-14  
9 age data and fracture coating data that provide important information regarding large-  
10 scale unsaturated flow processes in fractures and fracture-matrix interaction.

11

## 12 **Geological Setting**

13 Geological formations of the unsaturated zone of Yucca Mountain have been  
14 grouped into stratigraphic units (on the basis of welding) by Montazer and Wilson (1984).  
15 The stratigraphic units consist of the following, in descending order from the land surface:  
16 welded Tiva Canyon Tuff (TCw); mainly nonwelded Paintbrush Group (PTn); welded  
17 Topopah Spring Tuff (TSw); mostly nonwelded and sometimes altered Calico Hills  
18 Formation (CHn); and the mostly nonwelded and altered Crater Flat (undifferentiated)  
19 Group (CFu). The nonwelded zones near the water table in the CHn and CFu can be  
20 subject to zeolitic alteration that reduces the matrix permeability by orders of magnitude  
21 (Bandurraga and Bodvarsson, 1999). Furthermore, 35 hydrogeologic layers are defined to  
22 correspond to geologic formations and coincident hydrogeologic unit boundaries.

1 Welded formations are highly fractured, and nonwelded formations have relatively  
2 small fracture densities. Liquid water flow occurs mainly in the tuff matrix for nonwelded  
3 formations and in fractures for welded formations. Conceptual models of flow and  
4 transport in the unsaturated zone of Yucca Mountain can be found in Bodvarsson et al.  
5 (2001), Flint et al. (2001), and Liu (2000). For each of the 35 hydrogeologic layers,  
6 hydraulic properties include permeability and van Genuchten parameters for both fracture  
7 and matrix continua, with AFM parameter  $\gamma$  as an additional parameter. These properties  
8 are estimated by model calibration, based on small-scale property measurements, matrix  
9 saturation and potential data, and pneumatic data. The methodology of the model  
10 calibration has been reported in Bandurraga and Bodvarsson (1999), Liu et al. (1998) and  
11 Zhou et al. (2003).

12

### 13 **C-14 Data**

14

15 Carbon-14 data have been collected from perched water, pore water, and gas samples  
16 from the unsaturated zone of Yucca Mountain (Yang, 2002; Fabryka-Martin et al. 2000).  
17 Water travel times from ground surface to perched-water bodies were dominated by PTn,  
18 where flow occurs mainly in the rock matrix, and thus simulated water travel time to the  
19 groundwater table is insensitive to the AFM parameters. As a result, carbon-14 data  
20 collected from perched water are not used for validating the AFM. Pore-water carbon-14  
21 data from various boreholes at Yucca Mountain may not be representative of the pore-  
22 water residence time because of probable contamination by atmospheric  $^{14}\text{CO}_2$  during  
23 drilling, resulting in apparently younger residence times (Yang, 2002; Fabryka-Martin et

1 al. 2000). Carbon-14 data from gas samples are considered to be most representative of *in*  
2 *situ* conditions (Yang, 2002). Atmospheric  $^{14}\text{CO}_2$  during drilling is not expected to  
3 contaminate those gas samples collected several years after drilling. Gas samples were  
4 collected from two kinds of boreholes: open surface-based boreholes and instrumented  
5 (closed) surface-based boreholes. Because the data from the latter boreholes (USW SD-  
6 12 and USW UZ-1) are the most reliable indicators of *in situ* conditions (Fabryka-Martin  
7 et al. 2000), carbon-14 residence ages (Fabryka-Martin et al. 2000) calculated using the  
8 data from these two boreholes are used for validating the AFM.

9

10 Gas-phase carbon-14 ages are assumed to be representative of ages of the *in situ* pore  
11 water. The rationale for this assumption is provided in detail by Yang (2002). This  
12 assumption presumes rapid exchange of gas-phase  $\text{CO}_2$  (in hours to days) with dissolved  
13  $\text{CO}_2$  and  $(\text{HCO}_3^-)$  in pore water. Furthermore, the amount of C in an aqueous-phase  
14 reservoir relative to C in the  $\text{CO}_2$  gas-phase reservoir is a hundred times greater.  
15 Consequently, the aqueous phase will dominate the gaseous phase when exchange  
16 occurs, indicating the reasonableness of the assumption (Yang 2002).

17

### 18 **Fracture Coating Data**

19 The process of unsaturated-zone mineral deposition is initiated during infiltration  
20 where meteoric water interacts with materials in the soil, after which a portion may then  
21 enter the bedrock fracture network. Fracture coating is generally a signature of water flow  
22 paths. Thus, the coating data are useful for validating the AFM that describes water flow  
23 in fractures.

1

2 Fracture coating data were collected in an underground tunnel in the unsaturated zone  
3 of Yucca Mountain. Observed spatial distribution of fractures with coatings is used to  
4 estimate the portion of active fractures. For a given survey interval along the tunnel, a  
5 frequency of coated fractures can be estimated for a geologic unit based on the total  
6 number of coated fractures. The ratio of the coated fracture frequency to the total fracture  
7 frequency provides an estimate of portion of the active fracture for the given geologic  
8 unit. The estimated average portion of active fractures for the TSw is about 7.2 %. Note  
9 that fracture coatings may not precisely represent all the active flow paths in the  
10 unsaturated zone of Yucca Mountain (Liu et al., 1998). Nevertheless, these values give  
11 us at least an order-of-magnitude estimate of the portion of active fractures that is about  
12 10 %.

13

14 Mineral-coating growth rate data imply that the unsaturated zone fracture network has  
15 maintained a large degree of hydrologic stability over time, and that fracture flow paths  
16 in the deep unsaturated zone are buffered from climate-induced variations in precipitation  
17 and infiltration (Fabryka-Martin et al. 2000). If the AFM accurately represents water flow  
18 processes, modeling results based on the AFM should be consistent with this important  
19 observation.

20

## 21 **Comparison between Simulation Results and Field Observations**

22 One-dimensional dual-permeability numerical models are developed for boreholes  
23 USW SD-12 and USW UZ-1. Calibrated rock properties (Liu and Ahlers, 2003) are used,

1 except for  $\gamma$  values associated with the TSw formation, where the repository is proposed  
2 to be located. The value of the AFM parameter  $\gamma$  for the TSw formation is varied for  
3 different simulations to check the sensitivity of simulated water travel times to this  
4 parameter within the formation. The top boundary condition corresponds to the present-  
5 day infiltration rate for flow simulations and a constant tracer concentration for transport  
6 simulations. The initial condition for solute transport is zero concentration within the  
7 fractured rocks. Previous studies indicate that dispersion processes have an insignificant  
8 effect on overall solute transport behavior in unsaturated fractured rocks (Bodvarsson et  
9 al., 2000; Liu et al., 2003b), and therefore are ignored here. An effective-diffusion-  
10 coefficient value of  $1.97\text{E-}10 \text{ m}^2/\text{s}$  is employed, which is equal to the average value of  
11 coefficients for tritiated water measured from tuff matrix samples. TOUGH2 and T2R3D  
12 codes (Pruess, 1991; Wu et al., 1996) are used for simulating steady-state water flow and  
13 tracer transport processes. Liu et al. (2000) reported good agreement between simulation  
14 results using the above two codes for solute transport in the unsaturated zone of Yucca  
15 Mountain and those obtained using a particle tracking method without numerical  
16 dispersion, indicating that the effects of numerical dispersion are insignificant for the  
17 problem under consideration. Simulated water travel times (or ages) for rock matrix are  
18 compared with carbon-14 ages. A simulated water travel time at a location is determined  
19 as the time when the matrix concentration reaches 50% of the top-boundary  
20 concentration. It represents the average travel time for water particles from the ground  
21 surface to the location under consideration.

22 Fig. 3 shows simulated water travel times (ages) for different  $\gamma$  values of the TSw  
23 formation. Note that a major path for tracer transport into the tuff matrix is from

1 fractures to the tuff matrix, which is different from tracer transport processes within a  
2 single continuum. The considerable sensitivity of simulated results to  $\gamma$  indicates that  
3 carbon-14 data are useful for validating the AFM and for constraining the  $\gamma$  values for the  
4 TSw unit. For  $\gamma$  values ranging from 0.2 to 0.4, simulated results approximately match  
5 the observations for the two boreholes simultaneously, although a better match is  
6 obtained for USW SD-12 than that for USW UZ-14 (as a result of subsurface  
7 heterogeneity). In our current model, the heterogeneity within each geological layer is not  
8 considered. A larger  $\gamma$  value generally corresponds to a larger travel time (for the matrix),  
9 because of the smaller degree of matrix diffusion resulting from a smaller fracture-matrix  
10 interfacial area available for mass transport between fractures and the matrix (Eq. [10]).  
11 Note that the observed carbon-14 ages and simulated water travel times result from a  
12 combination of solute transport in fractures and the relatively slow matrix diffusion  
13 process. The spatial variability of the degree of matrix diffusion is the reason why the  
14 simulated water travel times and the observed ages in Fig. 3 are not always  
15 monotonically increasing with depth in the TSw.

16  
17 A sharp change in simulated water travel times occurs at an elevation of about 1,100 m  
18 for two boreholes (Fig. 3). This is because the upper portion of the TSw unit has  
19 relatively small fracture density values and therefore corresponds to a smaller degree of  
20 matrix diffusion for a given  $\gamma$  value. For the borehole USW UZ-1, simulated water travel  
21 time is generally longer than the observation for a given elevation. This may be owing to  
22 a subsurface heterogeneity that gives larger fracture densities (resulting in a larger degree  
23 of matrix diffusion) at the borehole location than what are used in the numerical model.

1 Layer-averaged fracture properties are used in the site-scale model of the unsaturated  
2 zone of Yucca Mountain. In general, a comparison between simulated water travel times  
3 and observed carbon-14 ages indicates that the AFM with  $\gamma$  values for the TSw between  
4 0.2 to 0.4 can reasonably represent the data.

5

6 To check the consistency of the AFM with the coating data, a one-dimensional model  
7 for borehole USW SD-12 is used. The model is the same as that described above. USW  
8 SD-12 is chosen because it is located near the middle of the underground tunnel where  
9 coating data were collected. Two infiltration rates (Flint et al., 1996), present day mean  
10 infiltration rate (3.4 mm/yr) and glacial maximum infiltration rate (17.3 mm/yr), are used  
11 for simulations. Again, uniform  $\gamma$  distributions for the TSw formation are employed. The  
12 latter infiltration rate is about five times as large as the former rate and represents the  
13 maximum infiltration rate in past climates.

14

15 Fig. 4 shows the simulated average portion of active fractures,  $f_a$ , for the TSw  
16 formation as a function of infiltration rate and  $\gamma$ . The average portion is calculated from  
17 Eq. [1] using the average effective saturation for the TSw formation. The calculated  $f_a$   
18 values are about 10 % to 40% for  $\gamma$  values ranging from 0.4 to 0.2 that are similar to those  
19 used for matching the carbon-14 data. Recall that the estimate of the active fracture  
20 portion from fracture coating data in the TSw was about 10%. Note that not all the active  
21 flow paths are associated with coatings and that coatings can also disappear due to  
22 dissolution. For example, Wang et al. (1999) found a flow feature under ambient  
23 conditions from the unsaturated zone of Yucca Mountain. This flow feature does not have

1 coatings. Therefore, coated fractures may represent the lower limit of the number of  
2 active fractures at the Yucca Mountain site. Since the number of active fractures  
3 increases with  $\gamma$ ,  $\gamma = 0.4$  may roughly represent the upper limit for the actual  $\gamma$  values. For  
4  $\gamma$  values less than 0.4, the calculated  $f_a$  values do not change significantly for the two  
5 infiltration rates (Figure 4), which is consistent with the observation of the stability of  
6 flow paths over time.

7

8 In summary, we have shown in this section that the AFM-based simulation results for  
9  $\gamma = 0.2 - 0.4$  approximately match the observed carbon-14 age data for the two borehole  
10 simultaneously. The similar range of  $\gamma$  value results in  $f_a$  values (for TSw) ranging from  
11 10% to 40%, consistent with the portion of active fracture (10%) estimated from the  
12 fracture coating data. This portion (10%) is believed to represent the lower limit for  $f_a$ , as  
13 previously discussed. The insensitivity of  $f_a$  values for  $\gamma = 0.2 - 0.4$  to infiltration rates is  
14 also consistent with the stability of flow paths over time that were observed from the  
15 unsaturated zone of Yucca Mountain. All these support the validity of the AFM.

16

17

### CONCLUDING REMARKS

18 Accurately modeling flow and transport processes in natural unsaturated systems is  
19 very difficult, largely because these processes are generally localized and associated with  
20 fingering and preferential flow paths. While the continuum approach is still the most  
21 feasible choice for many large-scale problems encountered in the real world, the  
22 traditional continuum approach has generally failed in capturing localized flow behavior,  
23 because of the use of volume averaging at a subgrid scale.

1

2 Two schools of thought exist regarding how to address the problem mentioned above.  
3 A number of researchers suggest using modeling approaches that are completely different  
4 from the continuum approach, such as the DLA and percolation-based approaches (e.g.,  
5 Ewing and Berkowitz, 2001; Glass 1993; Flury and Flühler 1995). These approaches  
6 have been successfully used to represent relatively small-scale observations. However,  
7 the use of these discrete approaches is very limited for large-scale applications.  
8 Furthermore, completely satisfactory theories underlying these approaches are still  
9 missing, and some critical steps in these approaches are somewhat arbitrary (Meakin and  
10 Tolman, 1989; Ewing and Berkowitz, 2001).

11

12 The other school of thought is to modify the continuum approach by incorporating  
13 key features of the discrete approaches (or small-scale observations), considering that the  
14 continuum approach is computationally efficient and robust, and often preferred for  
15 large-scale problems. Obviously, the AFM is a product of this school of thought. Note  
16 that although these discrete approaches have different physical origins, they are  
17 connected by the same class of flow patterns: fractals. Fractal flow behavior is also  
18 supported by field observations from different unsaturated systems, including the  
19 unsaturated zone of Yucca Mountain. Because of the relative simplicity of fractal-based  
20 characterizations, we believe that the key small-scale features in unsaturated systems can  
21 be successfully incorporated into large-scale continuum approaches. This is partially  
22 supported by the consistency between simulation results based on the AFM and a variety  
23 of field observations from the unsaturated zone of Yucca Mountain.

1  
2  
3  
4  
5  
6  
7  
8  
9  
10  
11  
12  
13  
14  
15  
16  
17  
18  
19  
20  
21  
22  
23

While we have demonstrated that the AFM is, in general, consistent with fractal flow behavior and can capture the major flow and transport features in the unsaturated zone of Yucca Mountain, more studies are needed to further improve it. For example, the AFM assumes a homogeneous distribution of flow field within the active-fracture continuum, whereas in reality the flow field may be very heterogeneous. One way to resolve this issue may be based on the concept of the multifractal (e.g., Feder 1988; Liu and Molz 1997). Another issue is that film flow is not explicitly considered in the current version of the AFM, while the film flow may be a potentially important mechanism of unsaturated flow in fractured rocks (Tokunaga and Wan, 1997). Note that the practical significance of film flow in unsaturated fractured rocks is still an issue of current debate (Tokunaga and Wan, 1997; Liu et al., 1998; Pruess et al., 1999; Or and Tuller, 2000; National Research Council, 2001). Field tests in the unsaturated zone of Yucca Mountain are also being currently performed with a major objective to further evaluate and improve the AFM. In the future, we will report on further evaluation of the AFM with data observed from these tests.

1  
2  
3  
4  
5  
6  
7  
8  
9  
10  
11  
12  
13  
14  
15  
16  
17  
18  
19  
20  
21  
22  
23  
24  
25  
26  
27  
28  
29  
30  
31

**Acknowledgment.** We are indebted to Q. Zhou and D. Hawkes at Lawrence Berkeley National Laboratory for their careful review of a preliminary version of this manuscript. We also thank two anonymous reviewers for their constructive comments. This work was supported by the Director, Office of Civilian Radioactive Waste Management, U.S. Department of Energy, through Memorandum Purchase Order EA9013MC5X between Bechtel SAIC Company, LLC, and the Ernest Orlando Lawrence Berkeley National Laboratory (Berkeley Lab). The support is provided to Berkeley Lab through the U.S. Department of Energy Contract No. DE-AC03-76SF00098.

1  
2  
3  
4  
5  
6  
7  
8  
9  
10  
11  
12  
13  
14  
15  
16  
17  
18  
19  
20  
21  
22  
23  
24  
25  
26  
27  
28  
29  
30  
31  
32  
33  
34  
35  
36  
37  
38  
39  
40  
41  
42  
43  
44  
45

## References

Bandurraga, T.M., and G.S. Bodvarsson. 1999. Calibrating hydrogeologic parameters for the 3-D site-scale unsaturated zone model of Yucca Mountain, Nevada. *J. Contam. Hydrol.* 38:47-46.

Bear, J., Tsang, C.F., de Marsily, G. (eds.). 1993. *Flow and Contaminant Transport in Fractured Rock*. Academic Press, San Diego, California.

Bodvarsson, G. S., and Y. Tsang, (Guest Editors). 1999. *Yucca Mountain Project*, *J. Contam. Hydrol.* 38:1-146.

Bodvarsson, G.S., H.H. Liu, R. Ahlers, Y.S. Wu and E. Sonnenthal. 2000. Parameterization and upscaling in modeling flow and transport at Yucca Mountain, in *Conceptual Models of Unsaturated Flow in Fractured Rocks*, National Academy Press, Washington, D.C..

Brooks, R. H., and Corey, A.T. 1964. Hydraulic properties of porous media. *Hydrol. Pap. No. 3*. Colorado State Univ., Fort Collins.

Buscheck T.A., N.D. Rosenberg, J. Gansemer and Y. Sun. 2002. Thermohydrologic behavior at an underground nuclear waste repository. *Water Resour. Res.* 10.1029/2000WR00010.

Doughty, C. 1999. Investigation of conceptual and numerical approaches for evaluating moisture, gas, chemical and heat transport in fractured rock. *J. Contam. Hydrol.* 38: 69-106.

Ewing, R. P. and B. Berkowitz. 2001. Stochastic pore-scale growth models of DNAPL migration in porous media. *Advances in Water Resources* 24:309-323.

Fabryka-Martin J., A. Meijer, B. Marshall, L. Neymark, J. Paces, J. Whelan and A. Yang. 2000. Analysis of geochemical data for the unsaturated zone. Rep. ANL-NBS-HS-000017. CRWMS M&O, Las Vegas, Nevada.

Feder J. 1988. *Fractals*. Plenum Press, New York.

Flint, A.L., L.E. Flint, G.S. Bodvarsson, E.M. Kwicklis and J. Fabryka-Martin. 2001. Development of the conceptual model of unsaturated zone hydrology at Yucca Mountain, Nevada. in *Conceptual Models of Unsaturated Flow in Fractured Rocks*, National Academy Press, Washington, D.C.

Flint, A.L., J. A. Hevesi, E.L. Flint. 1996. Conceptual and numerical model of infiltration for the Yucca Mountain area, Nevada, *Water Resources Investigation Report-96*. U.S. Geologic Survey, Denver, Co.

1  
2 Flury M. and H. Flühler. 1995. Modeling solute leaching in soils by diffusion-limited  
3 aggregation: Basic concepts and applications to conservative solutes. *Water Resour. Res.*  
4 31; 2443-2452.  
5  
6 Gerke, H.H. and M. Th. Van Genuchten, 1993. A dual-porosity model for simulating the  
7 preferential movement of water and solutes in structured porous media. *Water Resour.*  
8 *Res.* 29: 305-319.  
9  
10 Glass R.J. 1993. Modeling Gravity-Driven fingering using modified percolation theory.  
11 In Proceedings of the fourth annual international conference on high level radioactive  
12 waste conference, Las Vegas, Nevada.  
13  
14 Glass, R. J., M. J., Nicholl, and V. C., Tidwell. 1996. Challenging and improving  
15 conceptual models for isothermal flow in unsaturated, fractured rocks through  
16 exploration of small-scale processes. Rep. SAND95-1824, Sandia National Laboratories,  
17 Albuquerque, NM.  
18  
19 Ho, C.K., 1997. Models of fracture-matrix interactions during multiphase heat and mass  
20 flow in unsaturated fractured porous media. Sixth symposium on multiphase transport in  
21 porous media, ASME International Mechanical Engineering Congress and Exposition,  
22 Dallas, TX.  
23  
24 Karasaki, K., S., Segan, K., Pruess, and S., Vomvoris. 1993. A study of two-phase flow  
25 in fracture networks. in Proceedings of the Fifth Annual International High-Level  
26 Radioactive Waste Management Conference, Am. Nucl. Soc., La Grange, IL.  
27  
28 Kwicklis, E. M., and R.W. Healey. 1993. Numerical investigation of steady liquid water  
29 flow in a variably saturated fracture network. *Water Resour. Res.*, 29: 4091–4102.  
30  
31 Liu, H. H. and F.J. Molz. 1997. Multifractal analyses of hydraulic conductivity distribution.  
32 *Water Resour. Res.* 33: 2483-2488.  
33  
34 Liu, H. H., C. Doughty, and G. S. Bodvarsson. 1998. An active fracture model for  
35 unsaturated flow and transport in fractured rocks. *Water Resour. Res.* 34: 2633–2646.  
36  
37 Liu, H. H., G. S. Bodvarsson, and L. Pan. 2000. Determination of particle transfer in  
38 random walk particle methods for fractured porous media. *Water Resour. Res.* 36: 707-  
39 713.  
40  
41 Liu, H. H., and G. S. Bodvarsson. 2001. Constitutive relations for unsaturated flow in  
42 fracture networks. *J. of Hydrology.* 252: 116-125.  
43  
44 Liu, H.H., G.S. Bodvarsson and S. Finsterle. 2003a. A Note on unsaturated flow in two-  
45 dimensional fracture networks. *Water Resour. Res.* 38 (9), 1176,  
46 doi:10.1029/2001WR000977.

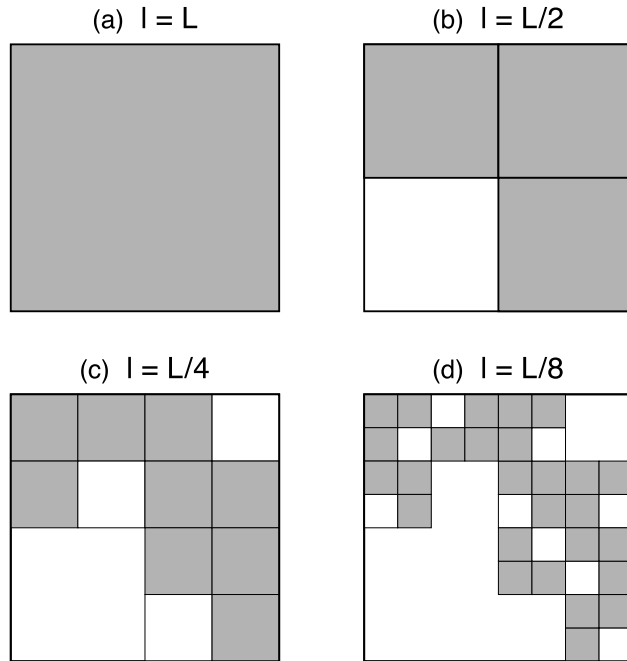
- 1  
2 Liu, H.H., C. B. Haukwa, F. Ahlers, G. S. Bodvarsson, A. L. Flint, and W. B. Guertal.  
3 2003b. Modeling flow and transport in unsaturated fractured rocks: An evaluation of the  
4 continuum approach. *J. Contam. Hydrol.* (in press).
- 5  
6 Liu, H.H. 2000. Conceptual and numerical models for UZ flow and transport. Rep. MDL-  
7 NBS-HS-000005, CRWMS M&O, Las Vegas, Nevada.
- 8  
9 Liu, H.H., and C.F. Ahlers. 2003. Calibrated properties model. Rep. MDL-NBS-HS-  
10 000003. BSC, Las Vegas, Nevada.
- 11  
12 Mandelbrot B. B. 1982. *The fractal geometry of nature.* W.H. Freeman, New York.
- 13  
14 Meakin P. and S. Tolman. 1989. Diffusion-limited aggregation. In *Fractals in the natural*  
15 *sciences.* Princeton Univ. Press, Princeton, N.J.
- 16  
17 Molz, F.J., and G.K. Boman. 1993. A stochastic interpolation scheme in subsurface  
18 hydrology. *Water Resour. Res.* 29 :3769-3774.
- 19  
20 Molz, F.J., H.H. Liu, and J. Szulga. 1997. Fractional Brownian motion and fractional  
21 Gaussian noise in subsurface hydrology: A review, presentation of fundamental  
22 properties, and extensions. *Water Resour. Res.* 33 : 2273-2286.
- 23  
24 Moridis G. and Q. Hu. 2000. Radionuclide transport model under ambient conditions.  
25 Rep. MNL-NBS-HS-000008, CRWMS M&O, Las Vegas, Nevada.
- 26  
27 Montazer P. and W.E. Wilson. 1984. Conceptual hydrologic model of flow in unsaturated  
28 zone, Yucca Mountain, Nevada. *Water-Resources Investigation Report 84-4345.* US  
29 Geologic Survey, Lakewood, CO.
- 30  
31 National Research Council. 1996. *Rock Fractures and Fluid Flow: Contemporary*  
32 *Understanding and Applications.* National Academy Press, Washington, D.C.
- 33  
34 National Research Council. 2001. *Conceptual Models of Unsaturated Flow in Fractured*  
35 *Rocks,* National Academy Press, Washington, D.C..
- 36  
37 Neuman, S.P. 1990. Universal scaling of hydraulic conductivities and dispersivities in  
38 geologic media. *Water Resour. Res.* 26: 1749-1758.
- 39  
40 Neuman, S.P. 1994. Generalized scaling of permeabilities: Validation and effect of support  
41 scale. *Geophys. Res. Lett.* 21:349-352.
- 42  
43 Or, D., and M. Tuller 2000. Flow in unsaturated fractured porous media: Hydraulic  
44 conductivity of rough surfaces. *Water Resour. Res.* 36:1165-1171.
- 45  
46 Perfect, E., N.B. McLaughlin, B.D. Kay, and G.C. Topp. 1996. An improved fractal  
47 equation for the soil water retention curve. *Water Resour. Res.* 32: 281-287.

- 1  
2 Paces, J. B., L.A. Newmark, B.D. Marshall, J.F. Whelan, and Z.E. Peterman. 1996. Ages  
3 and origins of subsurface secondary minerals in the Exploratory Studies Facility.  
4 Milestone Rep. 3GQH450M. U. S. Geol. Surv., Denver, Colo.  
5  
6 Persson M., H. Yasuda, J. Albergel, R. Berndtsson, P. Zante, S. Nasri, and P. Ohrstrom.  
7 2001. Modeling plot scale dye penetration by a diffusion limited aggregation (DLA)  
8 model. *J. Hydrol.* 250: 98-105.  
9  
10 Pruess, K. 1991. TOUGH2-A general purpose numerical simulator for multiphase fluid  
11 and heat flow. Rep. LBNL-29400. Lawrence Berkeley National Laboratory, Berkeley,  
12 CA.  
13  
14 Pruess, K., 1999. A mechanistic model for water seepage through thick unsaturated zones  
15 in fractured rocks of low matrix permeability. *Water Resour. Res.* 35: 1039-1051.  
16  
17 Pruess, K., B. Faybishenko, and G.S. Bodvarsson. 1999. Alternative concepts and  
18 approaches for modeling flow and transport in thick unsaturated zones of fractured rocks.  
19 *J. Contam. Hydrol.*, 38: 281-322.  
20  
21 Rasmussen, T.C. 1991. Steady fluid and travel times in partially structured fractures using  
22 a discrete air-water interface. *Water Resour. Res.* 27: 67-76.  
23  
24 Rieu, M., and G. Sposito. 1991a. Fractal fragmentation, soil porosity, and soil water  
25 properties, 1. Theory. *Soil Sci. Soc. Am. J.*, 55:1231-1238.  
26  
27 Rieu, M., and G. Sposito. 1991b. Fractal fragmentation, soil porosity, and soil water  
28 properties, 2. Applications. *Soil Sci. Soc. Am. J.*, 55: 1231-1238.  
29  
30 Robinson, B.A., A.V. Wolfsberg, H.S. Viswanathan, G. Bussod, C.W. Gable, and A.  
31 Meijer. 1997. The site-scale unsaturated zone transport model of Yucca Mountain. LANL  
32 milestone report SP25BMD.  
33  
34 Smith J.E. and Z. F. Zhang. 2001. Determining effective interfacial tension and  
35 predicting finger spacing for DNAPL penetration into water-saturated porous media. *J.*  
36 *Contam. Hydrol.* 48: 167-183.  
37  
38 Stauffer D. and Aharony, A. 1991. Introduction to Percolation Theory. Taylor & Francis.  
39  
40 Su, G.W., J.T. Geller, K. Pruess, and F. Wen. 1999. Experimental studies of water  
41 seepage and intermittent flow in unsaturated rough-walled fractures. *Water Resour. Res.*,  
42 35: 1019-1037.  
43  
44 Van Genuchten, M. 1980. A closed-form equation for predicting the hydraulic  
45 conductivity of unsaturated soil. *Soil Sci. Soc. Amer. J.* 44: 892-898.  
46

1 Tokunaga, T. K., and J. Wan. 1997. Water film flow along fracture surface of porous  
2 rock. *Water Resour. Res.* 33: 1287-1295.  
3  
4 Tyler, S.W., and S.W. Wheatcraft. 1990. Fractal processes in soil water retention. *Water*  
5 *Resour. Res.* 26:1047-1054.  
6  
7 Wang J.S.Y., R.C. Trautz, P.J. Cook, S. Finsterle, A.L. James and J. Birkholzer. 1999.  
8 Field tests and model analyses of seepage into drift. *J. Contam. Hydrol.* 38:232-347.  
9  
10 Wang Z., Feyen J., and Elrick D.E. 1998. Prediction of fingering in porous media. *Water*  
11 *Resources Research* 34:2183-2190.  
12  
13 Witten, T.A. and L. M. Sander. Diffusion-limited aggregation: A kinetic critical  
14 phenomenon. *Phys. Rev. Lett.* 47: 1400-1403.  
15  
16 Wilkinson D. and J.F. Willewsen. 1983. Invasion percolation: A new form of percolation  
17 theory. *J. Phys. A.* 16:3365-3376.  
18  
19 Wu Y. S., L. Pan, W. Zhang and G.S. Bodvarsson. 2002. Characterization of flow and  
20 transport processes within the unsaturated zone of Yucca Mountain, Nevada, under  
21 current and future climates. *J. of Hydrology.* 54: 215-247.  
22  
23 Wu, Y.S., J. Liu, T. Xu, C. Haukwa, W. Zhang, H.H. Liu, C.F. Ahlers. 2000. UZ flow  
24 models and submodels. Rep. MDL-NBS-HS-000006, CRWMS M&O, Las Vegas,  
25 Nevada.  
26  
27 Wu, Y. S., C.F. Ahlers, P. Fraser, A. Simmons, K. Pruess, 1996. Software qualification  
28 of selected TOUGH2 modules. LBNL-39490, Lawrence Berkeley National Laboratory,  
29 Berkeley, CA.  
30  
31 Xu T., E. Sonnenthal, and G. S. Bodvarsson. 2003. A reaction-transport model for calcite  
32 precipitation and evaluation of infiltration fluxes in unsaturated fractured rock. *J.*  
33 *Contam. Hydrol.* (in press).  
34  
35 Yamamoto H., K. Kojima and H. Tosaka, 1993. Fractal clustering of rock fractures and  
36 its modeling using cascade process. In *Scale Effects in Rock Masses 93*, Pinto da Cunha  
37 (ed.). 1993 Balkema, Rotterdam.  
38  
39 Yang, I.C. 2002. Percolation flux and transport velocity in the unsaturated zone, Yucca  
40 Mountain, Nevada. *Applied Geochemistry.* 17: 807-817.  
41  
42 Zhou Q., H.H. Liu, G.S. Bodvarsson, and C. M. Oldenburg. 2003. Flow and transport in  
43 unsaturated fractured rock: Effects of multiscale heterogeneity of hydrogeologic  
44 properties. *J. Contam. Hydrol.* 60: 1-30.  
45

Zimmerman, R.W., and G.S. Bodvarsson. 1996. Effective transmissivity of two-dimensional fracture networks. *Int. J. Rock Mech. Min. Sci.* 33: 433-438.

1  
2  
3  
4  
5  
6  
7  
8  
9  
10  
11  
12  
13  
14  
15  
16  
17  
18  
19  
20  
21  
22  
23  
24  
25  
26  
27  
28  
29  
30  
31  
32  
33  
34  
35  
36  
37  
38  
39  
40  
41  
42  
43  
44  
45  
46



AT03-002

1

2

**Fig. 1.** Demonstration of the “box” counting procedure for several box sizes

3

4

5

6

7

8

9

10

11

12

13

14

15

16

17

18

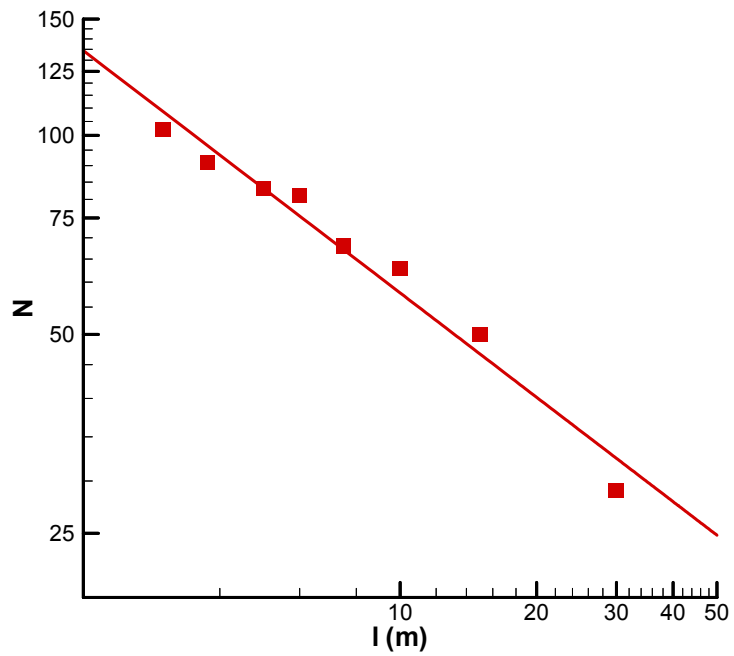
19

20

21

22

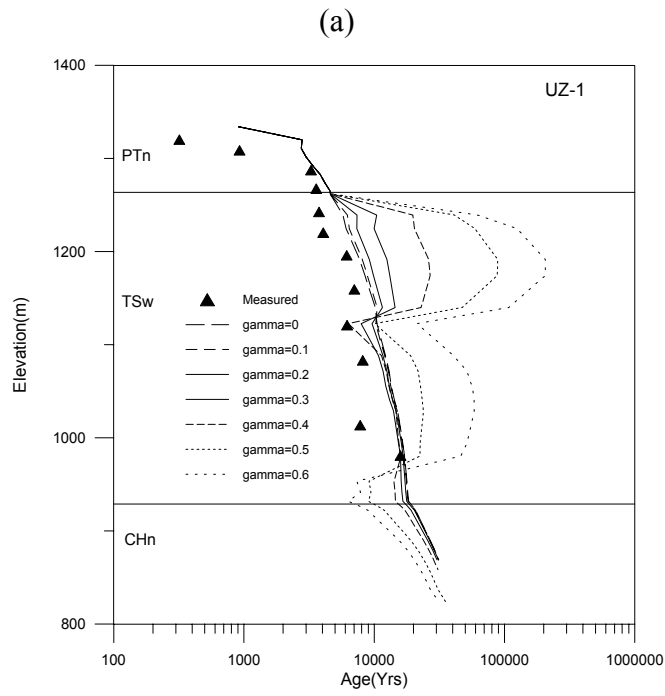
23



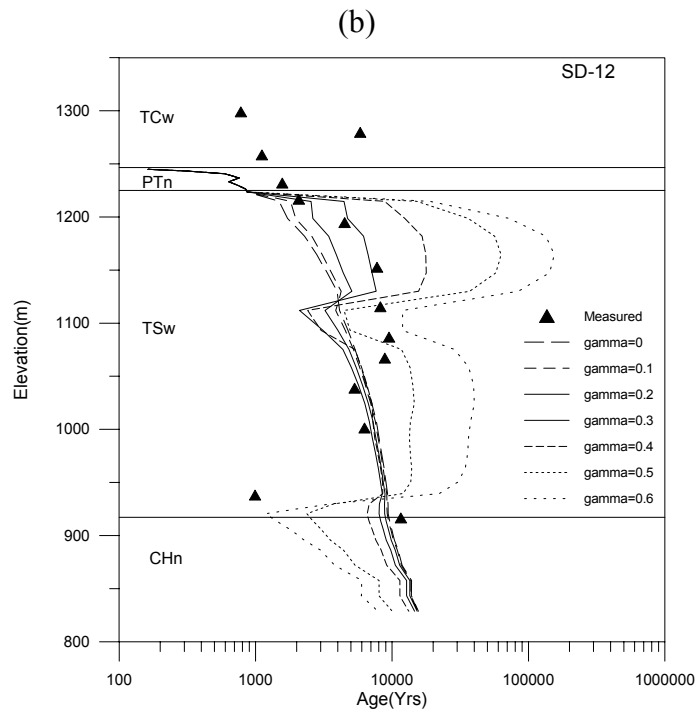
1  
2  
3  
4  
5  
6  
7  
8  
9  
10  
11  
12  
13  
14  
15  
16  
17  
18  
19  
20  
21  
22  
23  
24  
25  
26  
27

**Fig. 2.** Relation between the number of box ( $N$ ), covering at least one intersection between coated fractures and the survey line, as a function of box size  $l$ . The solid line corresponds to a power function (with a power of  $-0.5$ ) used to fit the data points.

1  
2



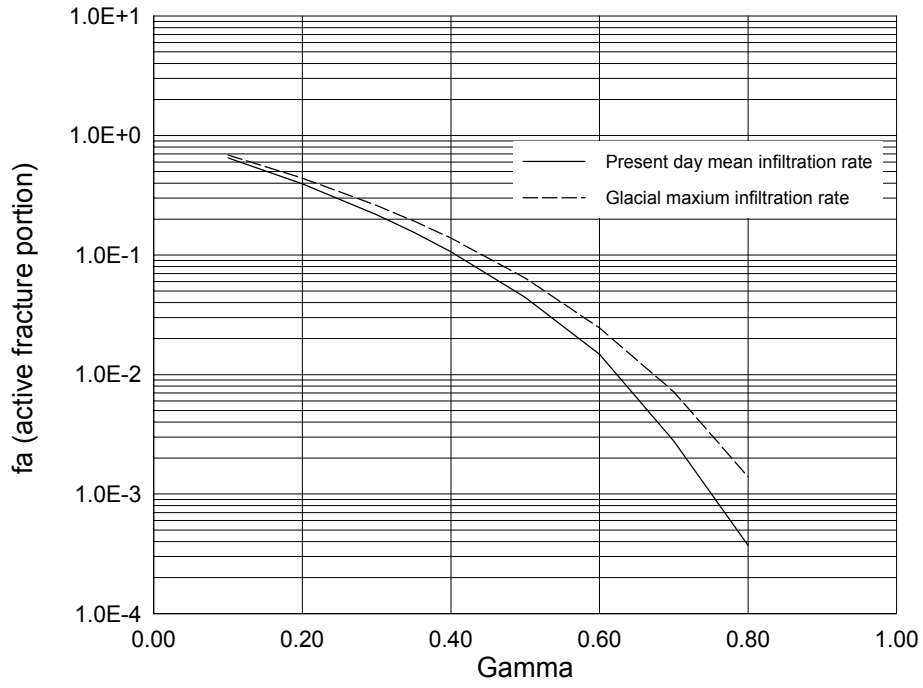
3  
4



5  
6  
7  
8  
9  
10  
11

**Figure 3.** Comparisons between simulated water travel times (ages) for rock matrix at boreholes (a) USW UZ-1 and (b) USW SD-12 and the corresponding Carbon-14 ages for several  $\gamma$  values.

1



2

3

4

**Fig. 4.** Simulated average portion of active fracture for the TSw formation as a function of infiltration rate and  $\gamma$ .

5

6

7

8

9